The EMBO Journal vol.15 no.23 pp.6400–6407, 1996

Dimerization of TWIK-1 K^+ channel subunits via a disulfide bridge

Florian Lesage, Roberto Reyes, Michel Fink, Fabrice Duprat, Eric Guillemare and Michel Lazdunski[1]

Institut de Pharmacologie Moléculaire et Cellulaire, CNRS, 660, route des Lucioles, Sophia Antipolis, 06560 Valbonne, France

[1]Corresponding author

F.Lesage and R.Reyes contributed equally to this work

TWIK-1 is a new type of K^+ channel with two P domains and is abundantly expressed in human heart and brain. Here we show that TWIK-1 subunits can self-associate to give dimers containing an interchain disulfide bridge. This assembly involves a 34 amino acid domain that is localized to the extracellular M1P1 linker loop. Cysteine 69 which is part of this interacting domain is implicated in the formation of the disulfide bond. Replacing this cysteine with a serine residue results in the loss of functional K^+ channel expression. This is the first example of a covalent association of functional subunits in voltage-sensitive channels via a disulfide bridge.

Keywords: baculovirus/interacting domain/ionic channels/mutagenesis/*Xenopus* oocyte

Introduction

K^+ channels are ubiquitous proteins whose activity is involved in the setting of the resting membrane potential as well as in the modulation of the electrical activity of cells. In excitable cells, K^+ channels influence action potential waveforms, firing frequency and neurotransmitter secretion (Rudy, 1988; Hille, 1992). In non-excitable cells, they are involved in hormone secretion, cell volume regulation and potentially in cell proliferation and differentiation (Lewis and Cahalan, 1995). Developments in electrophysiology have allowed the identification and the characterization of an astonishing variety of K^+ channels that differ in their biophysical properties, pharmacology, regulation and tissue distribution (Rudy, 1988; Hille, 1992). More recently, cloning efforts have shed considerable light on the mechanisms that determine this functional diversity. Furthermore, analyses of structure–function relationships have provided an important set of data concerning the molecular basis of the biophysical properties (selectivity, gating, assembly, etc.) and the pharmacological properties of cloned K^+ channels.

Functional diversity of K^+ channels arises mainly from the existence of a great number of genes coding for pore-forming subunits (>30 genes cloned to date in mammals) (Betz, 1990; Pongs, 1992; Salkoff *et al.*, 1992; Jan and Jan, 1994; Doupnik *et al.*, 1995; Deal *et al.*, 1996) as well as for other associated regulatory subunits (Rehm and Lazdunski, 1988; Aldrich, 1994; Attali *et al.*, 1995; Pongs, 1995; Rhodes *et al.*, 1995; Fink *et al.*, 1996b). Two main structural families of pore-forming subunits have been identified. The first one consists of subunits with a conserved hydrophobic core containing six transmembrane domains (TMDs). These K^+ channel α subunits participate in the formation of outward rectifier voltage-gated (Kv) and Ca^{2+}-dependent K^+ channels. The fourth TMD contains repeated positive charges involved in the voltage gating of these channels and hence in their outward rectification (Logothetis *et al.*, 1992; Bezanilla *et al.*, 1994). The second family of pore-forming subunits have only two TMDs. They are essential subunits of inward-rectifying (IRK), G-protein-coupled (GIRK) and ATP-sensitive (K_{ATP}) K^+ channels. The inward rectification results from a voltage-dependent block by cytoplasmic Mg^{2+} and polyamines (Matsuda, 1991; Lu and Mackinnon, 1994; Nichols *et al.*, 1996). A conserved domain, called the P domain, is present in all members of both families (Pongs, 1993; Heginbotham *et al.*, 1994; Mackinnon, 1995; Pascual *et al.*, 1995). This domain is an essential element of the aqueous K^+-selective pore. In both groups, the assembly of four subunits is necessary to form a functional K^+ channel (Mackinnon, 1991; Yang *et al.*, 1995). This suggests that the K^+ pore in all types of channels is formed by four P domains.

In both six TMD and two TMD pore-forming subunit families, different subunits coded by different genes can associate to form heterotetramers with new channel properties (Isacoff *et al.*, 1990; Ruppersberg *et al.*, 1990; Sheng *et al.*, 1993; Wang *et al.*, 1993; Duprat *et al.*, 1995; Krapivinsky *et al.*, 1995). A selective formation of heteropolymeric channels may allow each cell to develop the best K^+ current repertoire suited to its function. Pore-forming α subunits of Kv channels are classified into different subfamilies according to their sequence similarity (Chandy and Gutman, 1993). Tetramerization is believed to occur preferentially between members of each subgroup (Covarrubias *et al.*, 1991). The domain responsible for this selective association is localized in the N-terminal region and is conserved between members of the same subgroup (Li *et al.*, 1992; Babila *et al.*, 1994; Lee *et al.*, 1994; Shen and Pfaffinger, 1995; Xu *et al.*, 1995). This domain is necessary for hetero- but not homomultimeric assembly within a subfamily and prevents co-assembly between subfamilies. Recently, pore-forming subunits with two TMDs were also shown to co-assemble to form heteropolymers (Duprat *et al.*, 1995; Kofuji *et al.*, 1995; Krapivinsky *et al.*, 1995). This heteropolymerization seems necessary to give functional GIRKs. IRKs are active as homopolymers but also form heteropolymers (Fink *et al.*, 1996a). Expression studies of chimeras between IRK and GIRK indicate that the domain responsible for the tetramerization is probably N-terminal as in the case of Kv channels (Fink *et al.*, 1996a).

New structural types of K^+ channels from yeast and human were identified recently. These channels have two P domains in their functional subunit instead of only one for Kv, IRK and GIRK channels (Ketchum *et al.*, 1995; Lesage *et al.*, 1996a,b; Reid *et al.*, 1996). The yeast channel contains eight TMDs while the human channel (called TWIK-1) has four.

TWIK-1 is expressed widely in human tissues and is particularly abundant in heart and brain. TWIK-1 currents are time independent and weakly inwardly rectifying. These properties suggest that TWIK-1 channels are involved in the control of the background K^+ membrane conductance (Lesage *et al.*, 1996b). Results presented here show that the pore-forming TWIK-1 subunit forms a functional dimer. This dimer is covalently assembled via a disulfide bridge. The extracellular domain of TWIK-1, as well as the cysteine residues which are essential elements for the dimerization process, have been identified.

Results and discussion

Immunological characterization of TWIK-1

The baculovirus/Sf9 cells expression system (Summers and Smith, 1987) was chosen to express the cloned human TWIK-1 K^+ channel. The coding sequence of TWIK-1 was placed under the control of the polyhedrin promoter in the AcMNPV baculovirus to give the recombinant virus Bac-TWIK-1. Insect Sf9 cells were infected with Bac-TWIK-1 at a high m.o.i. (>10 viruses per cell) and expression of TWIK was tested 72 h after the infection. Cells were harvested and total protein lysates were prepared and analysed by immunoblot using affinity-purified rabbit antibodies (α-C) directed against the C-terminal part of the protein (Figure 1A). Under non-reducing conditions [in the absence of 2-mercaptoethanol (βME)], two major bands were detected with M_rs of 37 and 65–80 kDa, and a minor band with an M_r >97 kDa (Figure 1B). Under reducing conditions (i.e. in the presence of βME), two polypeptides were detected with M_rs of 37 and 40 kDa (Figure 1B). No signal was obtained either in reducing or non-reducing conditions from non-infected Sf9 cells (data not shown) or from control Sf9 cells infected with a recombinant baculovirus (Bac-IsK) expressing the human IsK K^+ channel subunit (Lesage *et al.*, 1993). The M_r of 37 kDa is in good agreement with the M_r of 38 kDa calculated from the known sequence of TWIK-1. When protein lysates were treated with *N*-glycopeptidase and *O*-glycopeptidase before immunoblotting, only the polypeptides with M_rs of 65 (Figure 1C) and 37 kDa (data not shown) were then detected, demonstrating that other bands correspond to glycosylated polypeptides.

The observation that the band moving at 65 kDa gives rise to a band moving at 37 kDa in the presence of the reducing agent βME strongly suggests that TWIK-1 can self-associate via a disulfide bond to form a dimer. However, the M_r of 65 kDa appears to be lower than the size expected for a dimer consisting of two 37 kDa subunits. This difference could simply be due to the limitations of the SDS–PAGE analysis in determining the exact M_r. To check this point, a vector was constructed to express *in vitro* a polypeptide corresponding to a covalent tandem of TWIK-1 subunits. Analysis of the size of this polypeptide by SDS–PAGE has revealed that it too has

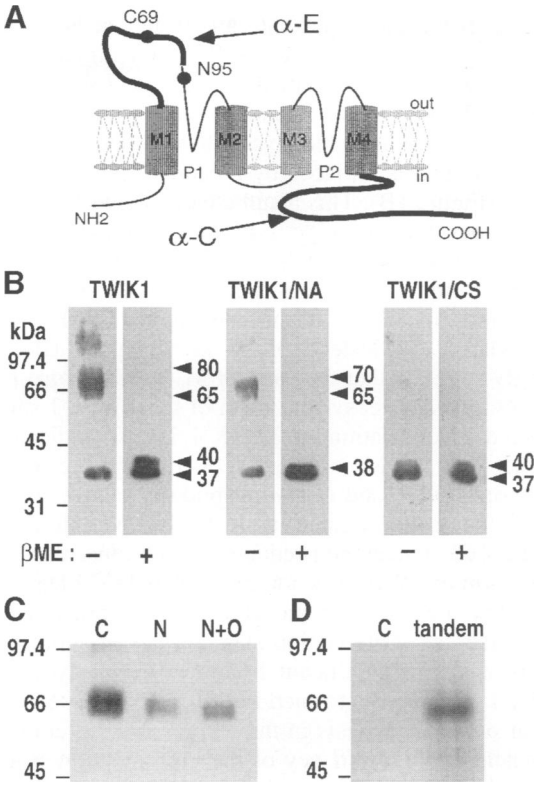

Fig. 1. Preparation of anti-TWIK-1 antibodies and immunological characterization of TWIK-1 from baculovirus-infected insect cells. (**A**) Rabbit antibodies were raised against the regions of TWIK-1 marked with a thick line. α-E antibodies are directed against the sequence from Pro47 to Val90 in the M1P1 linker loop and α-C against the sequence from Leu264 to His336 in the C-terminal region. This putative transmembrane orientation indicates the localization of Asn95 (the unique potential *N*-linked glycosylation site) and of Cys69. (**B**) Characterization of TWIK-1 from baculovirus-infected cells. Cell lysates were prepared 48 h after infection, and approximately equal amounts of proteins were separated by 9% SDS–PAGE and transferred onto a nitrocellulose membrane after treatment with (βME: +) or without (βME: –) 2-mercaptoethanol. The TWIK-1 and mutated TWIK-1 (TWIK-1/NA and TWIK-1/CS) polypeptides were detected by the α-C affinity-purified antibodies. Control, Sf9 cells infected with Bac-IsK; TWIK-1, Sf9 cells infected with Bac-TWIK-1; TWIK-1/NA, Sf9 cells infected with Bac-TWIK-1/NA; TWIK-1/CS, Sf9 cells infected with Bac-TWIK-1/CS. The molecular weight markers (in kilodaltons) are indicated on the left. (**C**) Effect of glycosidases on TWIK-1. Lane C, Sf9 membranes incubated in deglycosylation buffers but in the absence of enzymes; lane N, Sf9 membranes treated with *N*-glycopeptidase F; lane N+O, Sf9 membranes treated with *N*-glycopeptidase F and *O*-glycopeptidase. (**D**) *In vitro* translated TWIK-1 tandem. Lane C, control reaction without cRNA.

an M_r of 65 kDa (Figure 1D). On the other hand, the major TWIK-1 polypeptide immunoprecipitated from Sf9 cells infected by Bac-TWIK-1 in the presence of [^{35}S]-methionine also had an M_r of 65–80 kDa. Once reduced by βME, this form only gave rise to the expected bands of M_rs 37 and 40 kDa (data not shown). Therefore, the association of TWIK-1 with an endogenous protein of Sf9 cells seems to be excluded by all these results.

Only one consensus *N*-linked glycosylation site is present in the TWIK-1 protein and it lies in the M1P1 linker domain (N95) (Figure 1A). To test whether this site is used in cells to glycosylate TWIK-1, a recombinant baculovirus was constructed to express a mutant TWIK-1 subunit called Bac-TWIK-1/NA, in which Asn95 has been replaced by an alanine (N95A). Analysis of proteins

prepared from Bac-TWIK-1/NA-infected cells indicated that the apparent M_r of the TWIK-1/NA dimer is lower (65–70 kDa) than the M_r of the wild-type TWIK-1 dimer (Figure 1B). Furthermore, under reducing conditions, the band corresponding to the glycosylated monomer TWIK-1 (M_r of 40 kDa) is replaced by a band with a lower M_r of 38 kDa (Figure 1B). This result clearly shows that TWIK-1 undergoes *N*-linked glycosylation at N95. It also shows that the *N*-linked glycosylation of TWIK-1 is not necessary for the formation of the dimer. On the other hand, despite the suppression of this asparagine, TWIK-1 is still glycosylated (38 instead of 37 kDa, Figure 1B). This strongly suggests that the band of M_r 38 kDa corresponds to an *O*-linked glycosylated form of the TWIK-1 subunit. *O*-linked glycosylation of TWIK-1 is also indicated by the fact that the M_r of the TWIK-1 dimer treated with *N*-glycopeptidase and *O*-glycopeptidase is lower than the M_r of the dimer treated with *N*-glycopeptidase alone (Figure 1C). Under non-reducing conditions, the monomeric form of TWIK-1 is not glycosylated (37 kDa, Figure 1B). This suggests that the glycosylation process might occur after the dimerization step. However, another possibility is that a significant fraction of non-glycosylated TWIK-1 monomer is formed in Sf9 cells because the high rate of protein synthesis in this expression system cannot be matched by the efficacy of the glycosylation systems.

Which are the cysteines involved in the formation of interchain disulfide bridges in TWIK-1? Five of the nine cysteines are located in the putative TMDs, one in the N-terminal extremity of the protein, one in the C-terminal part, one in the P2 domain and one in the interdomain M1P1. It is well known that disulfide bridges are found preferentially in secreted proteins and on the extracellular side of membrane proteins because of the reducing properties of the cytosol. The topology previously proposed for TWIK-1 (Lesage *et al.*, 1996b; Figure 1A) indicates that the only cysteine expected to be localized on the extracellular side of the protein is Cys69 that is situated in the M1P1 linker domain. To check whether this residue is involved in the formation of an interchain disulfide bridge, a recombinant baculovirus was constructed to express a mutant TWIK-1 subunit called Bac-TWIK-1/CS in which this residue has been replaced by a serine (C69S). Analysis of proteins prepared from Bac-TWIK-1/CS-infected cells indicated that the usual band corresponding to the TWIK-1 dimer (M_r of 65–80 kDa) was no longer detected (Figure 1B). The migration profile of the TWIK-1/CS polypeptides detected under non-reducing conditions was exactly the same as the profile obtained after reduction of the wild-type TWIK-1 dimer (Figure 1B). This result indicates that Cys69 is involved in the formation of an interchain disulfide bridge.

Taken together, all these results strongly suggest that TWIK-1 subunits self-associate via a disulfide bridge to form a dimer that is glycosylated. The additional faint band with an M_r >97 kDa (Figure 1B) could correspond to aggregates of TWIK-1 dimers and/or monomers.

Extracellular localization of the M1P1 linker domain

The involvement of N95 in *N*-linked glycosylation and of C69 in the formation of disulfide bridges, together with the localization of these two residues to the interdomain M1P1, strongly suggests that this protein domain is extracellular. To demonstrate directly that this view is correct, affinity-purified rabbit antibodies (α-E) raised against a major part of this domain were prepared (Figure 1A) and used to detect the expression of TWIK-1 at the cell surface of non-permeabilized cells. Forty eight hours after infection, cells were incubated successively with affinity-purified α-E antibodies and fluorescein isothiocyanate (FITC)-conjugated secondary antibodies. Figure 2 shows that an intense fluorescent signal was observable at the cell surface of Bac-TWIK-1-infected Sf9 cells. No signal was obtained from non-infected Sf9 cells (data not shown) or from cells infected with Bac-IsK. Since cells were not permeabilized, the accessibility of α-E antibodies to their epitopes on TWIK-1 firmly establishes the extracellular localization of the M1P1 linker loop. The same experiment carried out with Sf9 cells infected either with Bac-TWIK-1/CS or with Bac-TWIK-1/NA has revealed that these two mutant forms of TWIK-1 are expressed at the cytoplasmic membrane (Figure 2). This indicates that processing of TWIK-1 at the cell membrane occurs in the absence of covalent dimerization but also that the *N*-linked glycosylation is not necessary for this step.

Role of the M1P1 linker in the assembly of TWIK-1 subunits

The absence of a signal peptide in the TWIK-1 sequence, the presence of two P domains each flanked by two transmembrane domains and the demonstrated extracellular localization of the M1P1 linker suggest a topology model in which only the linker domains M1P1, P1M2, M3P2 and P2M4 are extracellular, whereas the N- and C-termini and the linker M3M4 are intracytoplasmic. As already discussed, if this topology is correct, then only one cysteine is extracellular (C69) and the interchain disulfide should necessarily be formed between the Cys69 residues of the two TWIK-1 subunits. Because disulfide bridges would form spontaneously only when the two cysteine residues become close enough in a non-reducing medium, a working hypothesis is that the M1P1 linker domains have a spontaneous tendency to interact to favour the formation of the disulfide bridge. To test this point, a vector was constructed to express in *Escherichia coli* a fusion protein containing a large part of the M1P1 linker comprising 44 amino acids (Pro47–Val90) and called fragment *A*. This fragment was placed C-terminal to glutathione *S*-transferase (GST, 26 kDa) (GST–A, Figure 3). The construct was transfected into AD494, a *trxB*$^-$ bacterial strain that allows disulfide bond formation in the cytoplasm. After induction of the GST–*A* expression by using isopropyl-β-D-thiogalactopyranoside (IPTG), a soluble protein lysate was prepared and analysed by immunoblot using affinity-purified α-E antibodies. Under non-reducing conditions, two polypeptides were specifically detected with M_rs of 32 and 64 kDa (Figure 3). The larger form was not seen under reducing conditions. This result strongly suggests that two GST–*A* proteins associate via their fragment *A* and that a disulfide bond is formed between C69 residues. To exclude the participation of the GST sequence in this assembly as well as the possible association of GST–*A* with a hypothetical bacterial protein of 32 kDa, a second vector was constructed. This vector was designed to express a fusion protein (His6–*A*) con-

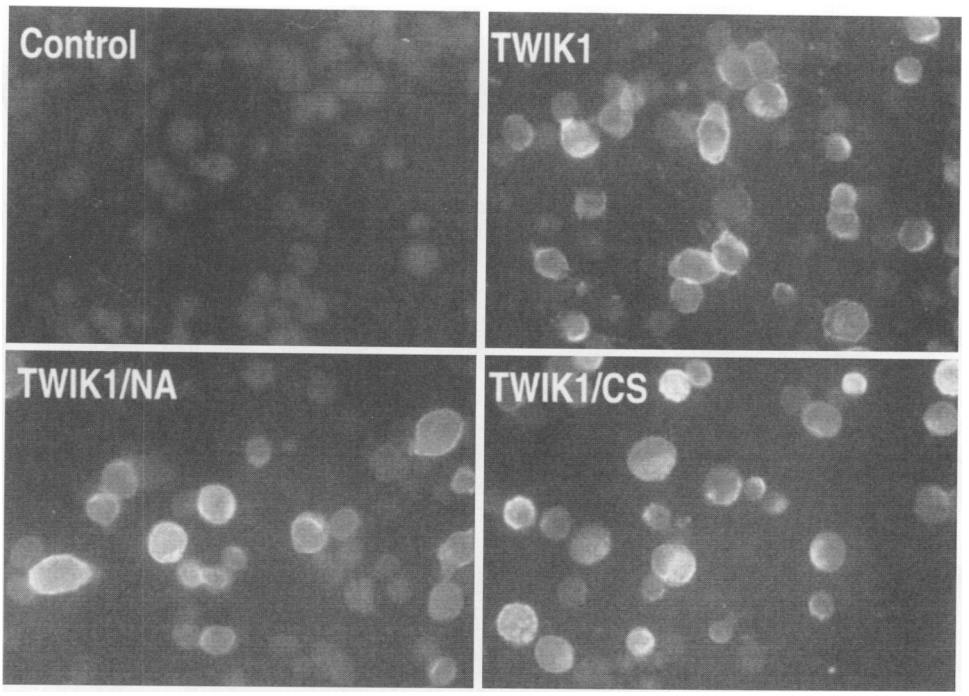

Fig. 2. Cell surface expression of the M1P1 domain of wild-type TWIK-1 and TWIK-1/NA and TWIK-1/CS mutants in baculovirus-infected insect cells. Cells were fixed with paraformaldehyde without permeabilization 48 h after infection and incubated successively with affinity-purified α-E antibodies and FITC-conjugated goat anti-rabbit IgG. Immunocomplexes were visualized by fluorescence microscopy at 400-fold magnification. Control, Sf9 cells infected with Bac-IsK; TWIK-1, Sf9 cells infected with Bac-TWIK-1; TWIK-1/NA, Sf9 cells infected with Bac-TWIK-1/NA; TWIK-1/CS, Sf9 cells infected with Bac-TWIK-1/CS.

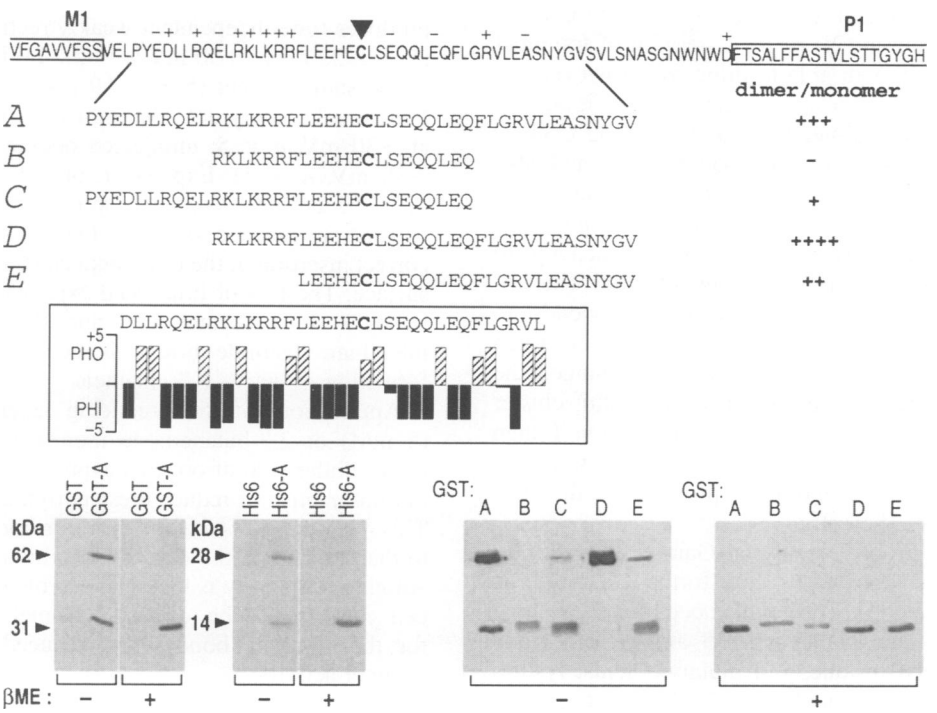

Fig. 3. Mapping of the self-interacting domain of TWIK-1. The sequence of the M1P1 linker domain is shown (first line of the upper panel). Charged residues and the Cys69 are indicated on this sequence. The assembly properties of various portions of this domain were assayed after their expression as GST or His6 fusion proteins. Fused fragments were: A, aa 47–90; B, aa 57–77; C, aa 47–77; D, aa 57–90; and E, aa 64–90 (upper panel). After induction of protein expression, bacteria were collected and lysed in Laemmli's buffer in the presence (+) or absence (–) of βME. Proteins were separated by 9% SDS–PAGE and fusion proteins were detected with α-E antibodies (lower panel). The relative abundance of dimer versus monomer observed under non-reducing conditions (n = 3) is indicated on the right of the upper panel. Inset, regular occurrence of large apolar and hydrophilic charged residues in the interacting domain. The predicted secondary structure of the core segment of the interacting domain is an α-helix (Asp50–Leu83). The hydropathy for single residues according to the Kyte and Doolittle scale (Kyte and Doolittle, 1982) is plotted below this segment. Hydrophobic residues (PHO) point upwards and hydrophilic ones (PHI) downwards.

taining the same region of the M1P1 linker as GST–*A* and an 83 amino acid sequence containing His6 and T7 tags, and a haemagglutinin epitope. From total proteins of transfected bacteria, α-E antibodies recognized polypeptides with M_rs of 14 and 28 kDa in the absence of βME and only the smaller form in the presence of βME (Figure 3). This result rules out a possible interaction of GST–*A* and His6–*A* with a bacterial protein. It can thus be concluded from these experiments that the fused M1P1 fragment of 44 amino acids is long enough to promote the physical self-association of two GST–*A* proteins followed by a covalent stabilization of the dimer arising via the formation of a disulfide bond between the two Cys69 residues. The presence of monomeric fusion proteins in addition to dimers could be explained by the fact that interactions between the TWIK-1 fragments and formation of the disulfide bridge are not favoured in the cytoplasm of bacteria.

In order to determine the minimum structure around Cys69 which is necessary for the interaction between the two M1P1 linker domains, different GST fusion proteins containing various portions of fragment *A* were expressed successively in bacteria. Fusion protein expression was induced by IPTG, and the soluble protein lysates were prepared. Self-association of the different forms was tested after separation of proteins by SDS–PAGE under non-reducing conditions, immunoblotting and detection with α-E antibodies. The results are shown in Figure 3. GST–*B*, a fusion protein corresponding to fragment *A* with a deletion of the 10 N-terminal and the 13 C-terminal amino acids, failed to self-associate. GST–*C* and GST–*D* (Figure 3) that retain the N- or the C-termini of fragment *A* respectively, were both able to dimerize. However, the extent of dimerization was not the same (Figure 3). GST–*C* produced less dimer than GST–*A* while GST–*D* gave higher amounts of dimers than GST–*C* and also GST–*A*. This result indicates that the C-terminal region plays an important role in the oligomeric assembly. The observation that GST–*D* retains a better capacity to dimerize than GST–*A* is not really understood. The last fusion protein tested was GST–*E*. It corresponds to GST–*D* with a deletion of a cluster of positively charged residues (RKLKRR). GST–*E* only partially retained the capacity to dimerize. This result indicates that this cluster of charged residues is involved in dimer formation. It then appears that a 34 amino acid domain of TWIK-1 (fragment *D*, Arg57–Val90) is large enough to promote the dimerization process very efficiently.

The secondary structure analysis (Garnier *et al.*, 1978) of fragment *A* predicts that its core forms a hydrophilic α-helix (Asp50–Leu83). The regular occurrence of large apolar residues (nine leucines in 35 amino acids) and hydrophilic charged residues (14 glutamic acids, lysines and arginines in 35 amino acids) is typical of interdigitating helices (Cohen and Parry, 1990) (Figure 3, inset). Self-dimerization of fragment *A* could be explained by hydrophobic interactions as well as specific ionic interactions between two identical helices. However, this domain does not present the rigorous heptad repeats with a leucine at every seventh position over a distance of several helical turns ('leucine zipper') that are found in molecules that form highly stabilized multimers.

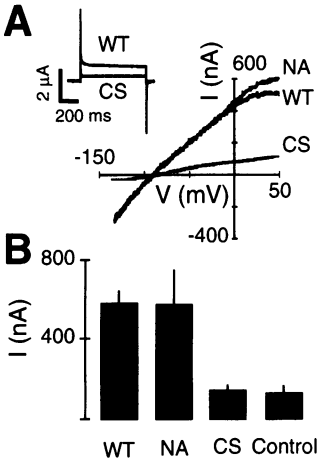

Fig. 4. Electrophysiology of TWIK-1, TWIK-1/NA and TWIK-1/CS in *Xenopus* oocytes. (**A**) Currents elicited by voltage ramps ranging from –130 to +50 mV (500 ms in duration) in oocytes injected with cRNAs coding for the TWIK-1 wild-type (WT) and for the TWIK-1/CS (CS) and TWIK-1/NA (NA) mutants. Inset: TWIK-1 WT and CS currents elicited by 800 ms long voltage steps to +30 mV. Recording were performed under two-microelectrode voltage-clamp with a holding potential of –80 mV (K^+ equilibrium potential). (**B**) Mean steady-state currents recorded at the end of voltage pulses as in (A). 'Control' refers to currents recorded from H_2O-injected oocytes. Vertical bars indicate the standard error of the mean (n = 5).

Electrophysiology of TWIK-1, TWIK-1/CS and TWIK-1/NA

Expression of TWIK-1 K^+ currents has been successfully achieved in *Xenopus* oocytes (Figure 4). TWIK-1 cRNA produces time-independent weakly rectifying K^+ currents (575 ± 22 nA at +30 mV, n = 5). TWIK-1/NA gave rise to the same current (568 ± 59 nA at +30 mV, n = 5). Functional activity was lost for TWIK-1/CS (140 ± 6 nA at +30 mV, n = 5; uninjected oocytes: 124 ± 9 nA at +30 mV, n = 5). Expression of TWIK-1/NA indicates that N95 and the *N*-linked glycosylation of the TWIK-1 subunit are not necessary for the processing and for the correct insertion of the functional channel at the membrane surface. The loss of functional expression of TWIK-1/CS strongly suggests that C69 and the formation of the interchain disulfide bridge is necessary for the stable formation of active K^+ channels.

Application of the reducing agents dithiothreitrol (5 mM) or 2,3-butanedione monoxime (2 mM) on the extracellular side of oocytes expressing TWIK-1 currents did not abolish or reduce these currents (data not shown). This result suggests that the disulfide bond is not accessible to these agents in the native conformation of the channel. Another possibility is that, once formed and present at the cell membrane, the dimeric channel is stable enough for the disulfide bond to be reduced with no loss of channel activity.

A structural model for TWIK-1 K^+ channels

TWIK-1 is a novel type of pore-forming K^+ channel subunit with four TMDs and two P domains. As a first step in understanding the structure and the function of TWIK-1, this protein has been expressed heterologously in insect cells by using the baculovirus expression system. The immunological characterization of the expressed TWIK-1 subunits strongly suggests that they self-associate

to give a homodimer containing an interchain disulfide bridge. The same dimerization has been obtained in transiently transfected COS cells, indicating that self-association of TWIK-1 to form a dimer is not dependent on the expression system used (our unpublished data). Mutagenesis experiments have shown that Cys69 localized in the extracellular M1P1 linker loop of TWIK-1 is involved in the formation of the interchain disulfide bond and that this residue is necessary for channel function.

Fusion proteins containing a large region of the M1P1 linker domain and Cys69 are able to associate as homodimers with the formation of a disulfide bridge implicating Cys69. A further deletion analysis of the M1P1 domain has shown that a region of only 34 amino acids (from Arg57 to Val90) contains structural elements for the dimerization of TWIK-1. This region is expected to form an amphipatic α-helix containing regularly spaced charged and hydrophobic residues. The dimeric association could then be explained easily by both hydrophobic and ionic interactions.

These results demonstrate that TWIK-1 subunits form homodimers. In the case of voltage-gated and inward rectifier K^+ channels, the functional channel is a tetramer containing four P domains that are involved in the formation of the K^+-selective pore (Mackinnon, 1991; Yang *et al.*, 1995). If both P domains in the TWIK-1 subunit are functional, then the active TWIK-1 K^+ channel is expected to be the disulfide-bridged homodimer. The first domain (P1) is probably functional because it is well conserved and contains all residues which have been shown to be necessary for the K^+ selectivity (Heginbotham *et al.*, 1994; Lesage *et al.*, 1996b). The second one (P2) is not so well conserved and contains an unusual motif (GLG instead of GY/FG). If this motif GLG is replaced by GIG or GYG by site-directed mutagenesis, the channel activity is lost, while if it is replaced by GFG, the channel activity is conserved (our unpublished data). This indicates that the motif GLG in the P2 domain is important for channel function. This does not provide a demonstration that both P1 and P2 loops participate in the pore formation. However, in light of what is known about K^+-selective pores for other type of channels, these results are a strong indication of such a participation. Another solid argument for this is the existence of sequences related to TWIK-1 and containing two P domains in the nematode *Caenorhabditis elegans* (Ketchum *et al.*, 1995; Lesage *et al.*, 1996b). Conservation of this structural arrangement during a long period in evolution between invertebrates and vertebrates is probably associated with a functional role for both P domains. Although the possibility that two dimers associate to form an active tetramer cannot be ruled out, the most likely hypothesis is that TWIK-1 homodimers are functional K^+ channels.

Figure 5 presents a possible model for the TWIK-1 channel structure. It is a protein consisting of a ring of eight transmembrane segments with, inside, an aqueous K^+-selective pore formed by the four P domains. In this model, two M1P1 linker loops are tightly associated and form an extracellular domain containing a disulfide bridge. Two sites of *N*-linked glycosylation are present in this domain. It is the cytoplasmic and hydrophilic N-terminal domains of Kv subunits that provide the molecular information for the co-assembly of these subunits (Li

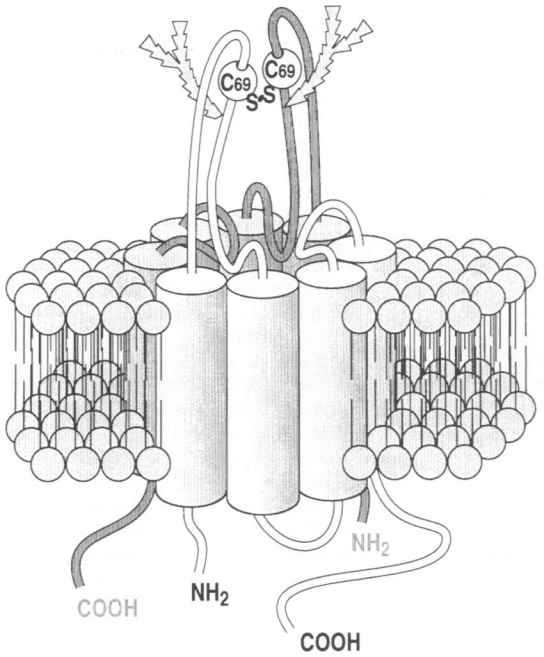

Fig. 5. A topological model for the TWIK-1 K^+ channel. The presence of two P domains in TWIK-1 and the capacity of this pore-forming K^+ channel subunit to dimerize suggest a working model in which the active TWIK-1 channel consists of two subunits, forming a ring of eight transmembrane segments with an inside K^+-selective aqueous pore formed by four P domains. The two M1P1 linker loops are tightly associated and form an extracellular domain containing an interchain disulfide bridge and two *N*-linked glycosylation sites.

et al., 1992; Babila *et al.*, 1994; Lee *et al.*, 1994; Shen and Pfaffinger, 1995; Xu *et al.*, 1995). It is also the hydrophilic and cytoplasmic N-terminal domains that are important for Kir assembly (Fink *et al.*, 1996a). For TWIK-1 the major interacting domain appears to be in the extracellular loop. However, the association of TWIK-1 subunits to form a dimer might also be driven by cytoplasmic segments of TWIK-1 such as the N-terminus.

The assembly of TWIK-1 dimers, unlike the assembly of Kv or Kir tetramers, requires the formation of a stabilizing interchain disulfide bridge. This is the first time that such a covalent association of subunits of voltage-sensitive channels has been reported. A covalent association also exists in voltage-sensitive Na^+ and Ca^{2+} channels. These channels are large structures with four repeated domains, each containing one P domain. However, in Na^+ and Ca^{2+} channels the different repeated domains are covalently assembled via peptide bonds.

Materials and methods

Preparation of affinity-purified antibodies

The rabbit polyclonal antibodies α-C directed against the C-terminal region of TWIK-1 (amino acids 264–336) and α-E directed against the M1P1 linker domain of TWIK-1 (amino acids 47–90) were raised against GST fusion proteins containing the corresponding fragments of TWIK-1 (see below for preparation and purification of the GST proteins). New Zealand female rabbits were immunized with 300 μg of purified proteins, in the presence of complete Freund's adjuvant, and boosted 1 month later with 150 μg of the immunogen in the presence of incomplete Freund's adjuvant. Rabbits were bled 15 days after the boost. The antibodies were affinity purified by using His–Tag fusion proteins containing the same domains of TWIK-1 as the GST fusion proteins used for the immunization (see below for the preparation and the purification of His–Tag fusion proteins). Briefly, the crude antisera were

incubated for 4 h at 4°C with 100–200 μg of His–Tag fusion proteins previously transferred to Hybond C-extra nitrocellulose membranes (Amersham). After three washes in phosphate-buffered saline [PBS; 10 mM phosphate buffer (pH 7.2), 0.15 M NaCl], 0.1% Tween 20, the anti-TWIK-1 antibodies were recovered by a 1 min elution of each strip with 0.1 M glycine, 0.5% bovine serum albumin (BSA), pH 2.8. After the elution, the purified antibodies were brought rapidly to pH 7.6 with 1 M Tris (pH 8.0), 0.5% BSA.

Sf9 baculovirus expression system

The pVL-TWIK-1 transfer vector was constructed by transferring the TWIK-1 coding sequence from the *Xenopus* oocyte expression vector pEXO-TWIK-1 to the pVL1392 vector (Pharmingen). pEXO-TWIK-1/NA and pEXO-TWIK-1/CS were obtained by amplifying the complete pEXO-TWIK-1 plasmid with a high fidelity DNA polymerase (Pwo DNA pol, Boehringer) and a pair of adjacent primers, one of them introducing a point mutation in the coding sequence of TWIK-1 (N95A and C69S, respectively). The PCR products were circularized and transformed into bacteria. The full TWIK-1/NA and TWIK-1/CS coding sequences were verified by sequencing on both strands before being subcloned into pVL1392 to give pVL-TWIK-1/NA and pVL-TWIK-1/CS. The three TWIK-1 transfer vectors were co-transfected individually with linearized baculovirus DNA (BaculoGold, Pharmingen) into Sf9 cells following the manufacturer's recommendations. Supernatants containing the recombinant viruses (Bac-TWIK-1, Bac-TWIK-1/NA and Bac-TWIK-1/CS) were harvested 96 h after the transfection. Expression of TWIK-1, TWIK-1/NA and TWIK-1/CS proteins in infected Sf9 cells was verified by immunoblot analysis of total proteins (see below). The protocols for Sf9 cell culture, viral infection and protein expression were identical to those described previously (Lesage *et al.*, 1993).

Immunofluorescence

At 48 h after the infection, Sf9 cells on coverslips were washed three times in PBS containing 1 mM $MgCl_2$ and 1 mM $CaCl_2$ then fixed in the same buffer containing 4% paraformaldehyde for 15 min at room temperature. After three washes with PBS, non-specific protein binding sites were blocked with PBS supplemented with 5% normal goat serum, 2% BSA for 1 h at room temperature, then incubated with affinity-purified α-E antibodies (1:100) for 1 h at room temperature. Cells were washed three times with PBS and incubated with FITC-conjugated goat anti-rabbit IgG (1:10 000) (Jackson) for 1 h at room temperature. Immunocomplexes were visualized by fluorescence microscopy.

Preparation of T7 expression vectors, protein expression and purification

DNA sequences coding for fragments of the M1P1 linker domain (P47–V90) and the C-terminal region (L264–H336) of TWIK-1 were amplified with a low error rate DNA polymerase (Pwo DNA pol, Boehringer). These DNA fragments were subcloned into pGEX3x (Pharmacia) 3′ to the coding sequence of GST or into a plasmid derived from pET3a (Novagen) 3′ to the His–Tag coding sequence. Plasmids were transformed into *E.coli* BL21pLysS. Isolated colonies were picked and allowed to grow in LB medium (100 μM ampicillin) to an OD_{600} of 0.7. At this stage, the fusion protein expression was induced by adding 1 mM IPTG for 4 h at 37°C. GST and His–Tag fusion proteins were then affinity-purified with glutathione–Sepharose (Pharmacia) or Ni-NTA (Quiagen) resins respectively, using the protocols provided by the manufacturers. To study the interaction properties of the M1P1 linker domain, several other GST fusion proteins were constructed. DNA fragments were amplified from TWIK-1 by PCR using primers designed to introduce *Bam*HI and *Eco*RI restriction sites at the 5′ and 3′ ends, respectively. After digestion, PCR products were inserted into pGEX3X linearized by *Bam*HI–*Eco*RI. Plasmids were verified by partial sequencing and transformed into the AD494 *E.coli* strain. The protein expression was induced by addition of 1 mM IPTG for 4 h at 37°C.

Protein preparation and immunodetection

Baculovirus-infected Sf9 cells were harvested 72 h after infection. Cells were washed three times with PBS and scraped at 4°C into a buffer consisting of 20 mM Tris (pH 7.4), 140 mM NaCl, 1 mM phenylmethylsulfonyl fluoride and 0.1 mM iodoacetamide. The cell suspension was homogenized with a cell disrupter (Vibra cell 72423, bioblock Scientific) set at a potency of 5 W. The insoluble material was removed by centrifugation at 12 000 *g* for 15 min at 4°C. Deglycosylation of Sf9 membrane proteins was performed as previously described (Lesage *et al.*, 1993). For bacterial fusion proteins, cells were collected and lysed directly in Laemmli's sample buffer. This sample buffer was prepared with or without βME in order to detect the presence of interchain disulfide bridges.

Proteins were separated on SDS–polyacrylamide gel and transferred to nitrocellulose membranes (Hybond C-extra, Amersham). Non-specific binding to the membrane was blocked by PBS supplemented with 0.1% Tween 20, 5% non-fat dry milk for 1 h at room temperature. The membranes were incubated overnight at 4°C with affinity-purified α-C or α-E antibodies (1:1000) and washed with PBS containing 0.1% Tween 20. The binding of the primary antibodies was detected by adding goat anti-rabbit horseradish peroxidase-conjugated secondary antibodies (1:10 000) (Jackson) for 1 h at room temperature, followed by enhanced chemiluminescence (ECL, Amersham) detection.

Construction of a TWIK-1 tandem DNA and in vitro translation

The covalent tandem TWIK-1 DNA was constructed in pBluescript by linking two sequences coding for TWIK-1 with a sequence encoding a 10 glutamine linker. This construct was verified by sequencing, then linearized and used as template for *in vitro* transcription. Synthesized cRNA was used for an *in vitro* translation experiment using rabbit reticulocyte lysate in the presence of [^{35}S]methionine according to the manufacturer's protocol (Promega).

Electrophysiological measurements

The pEXO-TWIK-1, pEXO-TWIK-1/CS and pEXO-TWIK-1/NA plasmids were linearized by *Bam*HI, and capped cRNAs were synthesized by using the T7 RNA polymerase (Stratagene). Preparation of *Xenopus laevis* oocytes and cRNA injection have been described elsewhere (Guillemare *et al.*, 1992). In a 0.3 ml perfusion chamber, a single oocyte was impaled with two standard glass microelectrodes (0.5–2.0 MΩ) filled with 3 M KCl and maintained under voltage clamp using a Dagan TEV200 amplifier. The bathing solution contained 96 mM NaCl, 2 mM KCl, 1.8 mM $CaCl_2$, 2 mM $MgCl_2$ and 5 mM HEPES at pH 7.4 with KOH. Stimulation of the preparation, data acquisition and analyses were performed using pClamp software (Axon instruments, USA).

Acknowledgements

We thank Drs J.Barhanin and G.Romey for very helpful discussions, D.Doume for secretarial assistance and F.Aguila for help with artwork. This work was supported by the Centre National de la Recherche Scientifique (CNRS), and the Ministère de l'Enseignement Supérieur et de la Recherche (contract MESR ACC SV9 No. 9509 113). Thanks are due to Bristol Myers Squibb Company for an 'Unrestricted Award'.

References

Aldrich,R.W. (1994) Potassium channels—new channel subunits are a turn-off. *Curr. Biol.*, **4**, 839–840.

Attali,B., Latter,H., Rachamim,N. and Garty,H. (1995) A corticosteroid-induced gene expressing an 'IsK-like' K^+ channel activity in *Xenopus* oocytes. *Proc. Natl Acad. Sci. USA*, **92**, 6092–6096.

Babila,T., Moscucci,A., Wang,H.Y., Weaver,F.E. and Koren,G. (1994) Assembly of mammalian voltage-gated potassium channels—evidence for an important role of the first transmembrane segment. *Neuron*, **12**, 615–626.

Betz,H. (1990) Homology and analogy in transmembrane channel design: lessons from synaptic membrane proteins. *Biochemistry*, **29**, 3591–3599.

Bezanilla,F., Perozo,E. and Stefani,E. (1994) Gating of *Shaker* K^+ channels. 2. The components of gating currents and a model of channel activation. *Biophys. J.*, **66**, 1011–1021.

Chandy,K.G. and Gutman,G.A. (1993) Nomenclature for mammalian potassium channel genes. *Trends Pharmacol. Sci.*, **14**, 434.

Cohen,C. and Parry,A.D. (1990) α-Helical coiled coils and bundles: how to design an α-helical protein. *Proteins*, **7**, 1–15.

Covarrubias,M., Wei,A. and Salkoff,L. (1991) *Shaker*, *Shal*, *Shab*, and *Shaw* express independent K^+ current systems. *Neuron*, **7**, 763–773.

Deal,K.K., England,S.K. and Tamkun,M.M. (1996) Molecular physiology of cardiac potassium channels. *Physiol. Rev.*, **76**, 49–67.

Doupnik,C.A., Davidson,N. and Lester,H.A. (1995) The inward rectifier potassium channel family. *Curr. Opin. Neurobiol.*, **5**, 268–277.

Duprat,F., Lesage,F., Guillemare,E., Fink,M., Hugnot,J.P., Bigay,J., Lazdunski,M., Romey,G. and Barhanin,J. (1995) Heterologous multimeric assembly is essential for K^+ channel activity of neuronal

and cardiac G-protein-activated inward rectifiers. *Biochem. Biophys. Res. Commun.*, **212**, 657–663.

Fink,M., Duprat,F., Heurteaux,C., Lesage,F., Romey,G., Barhanin,J. and Lazdunski,M. (1996a) Dominant negative chimeras provide evidence for homo and heteromultimeric assembly of inward rectifier K^+ channel proteins via their N-terminal end. *FEBS Lett.*, **378**, 64–68.

Fink,M., Duprat,F., Lesage,F., Heurteaux,C., Romey,G., Barhanin,J. and Lazdunski,M. (1996b) A new K^+ channel β subunit to specifically enhance Kv2.2 (CDRK) expression. *J. Biol. Chem.*, **271**, 26431–26438.

Garnier,J., Osguthrope,D. and Robson,B. (1978) Analysis of the accuracy and implications of simple methods for predicting the secondary structure of globular proteins. *J. Mol. Biol.*, **120**, 97–120.

Guillemare,E., Honore,E., Pradier,L., Lesage,F., Schweitz,H., Attali,B., Barhanin,J. and Lazdunski,M. (1992) Effects of the level of messenger RNA expression on biophysical properties, sensitivity to neurotoxins, and regulation of the brain delayed-rectifier K^+ channel Kv1.2. *Biochemistry*, **31**, 12463–12468.

Heginbotham,L., Lu,Z., Abramson,T. and Mackinnon,R. (1994) Mutations in the K^+ channel signature sequence. *Biophys. J.*, **66**, 1061–1067.

Hille,B. (1992) *Ionic Channels of Excitable Membranes*. 2nd edn. Sinauer, Sunderland, MA.

Isacoff,E.Y., Jan,Y.N. and Jan,L.Y. (1990) Evidence for the formation of heteromultimeric potassium channels in *Xenopus* oocytes. *Nature*, **345**, 530–534.

Jan,L.Y. and Jan,Y.N. (1994) Potassium channels and their evolving gates. *Nature*, **371**, 119–122.

Ketchum,K.A., Joiner,W.J., Sellers,A.J., Kaczmarek,L.K. and Goldstein,S.A.N. (1995) A new family of outwardly rectifying potassium channel proteins with two pore domains in tandem. *Nature*, **376**, 690–695.

Kofuji,P., Davidson,N. and Lester,H.A. (1995) Evidence that neuronal G-protein-gated inwardly rectifying K^+ channels are activated by G beta gamma subunits and function as heteromultimers. *Proc. Natl Acad. Sci. USA*, **92**, 6542–6546.

Krapivinsky,G., Gordon,E.A., Wickman,K., Velimirovic,B., Krapivinsky,L. and Clapham,D.E. (1995) The G-protein-gated atrial K^+ channel I-KACh is a heteromultimer of two inwardly rectifying K^+-channel proteins. *Nature*, **374**, 135–141.

Kyte,J. and Doolittle,R. (1982) A simple model for displaying the hydropathic character of a protein. *J. Mol. Biol.*, **157**, 105–106.

Lee,T.E., Philipson,L.H., Kuznetsov,A. and Nelson,D.J. (1994) Structural determinant for assembly of mammalian K^+ channels. *Biophys. J.*, **66**, 667–673.

Lesage,F., Attali,B., Lakey,J., Honore,E., Romey,G., Faurobert,E., Lazdunski,M. and Barhanin,J. (1993) Are *Xenopus* oocytes unique in displaying functional IsK channel heterologous expression? *Receptors Channels*, **1**, 143–152.

Lesage,F., Guillemare,E., Fink,M., Duprat,F., Lazdunski,M., Romey,G. and Barhanin,J. (1996a) A pH-sensitive yeast outward rectifier K^+ channel with two pore domains and novel gating properties. *J. Biol. Chem.*, **271**, 4183–4187.

Lesage,F., Guillemare,E., Fink,M., Duprat,F., Lazdunski,M., Romey,G. and Barhanin,J. (1996b) TWIK-1, a ubiquitous human weakly inward rectifying K^+ channel with a novel structure. *EMBO J.*, **15**, 1004–1011.

Lewis,R.S. and Cahalan,M.D. (1995) Potassium and calcium channels in lymphocytes. *Annu. Rev. Immunol.*, **13**, 623–653.

Li,M., Jan,Y.N. and Jan,L.Y. (1992) Specification of subunit assembly by the hydrophilic amino-terminal domain of the *Shaker* potassium channel. *Science*, **257**, 1225–1230.

Logothetis,D.E., Movahedi,S., Satler,C., Lindpaintner,K. and Nadalginard,B. (1992) Incremental reductions of positive charge within the S4 region of a voltage-gated K^+ channel result in corresponding decreases in gating charge. *Neuron*, **8**, 531–540.

Lu,Z. and Mackinnon,R. (1994) Electrostatic tuning of Mg^{2+} affinity in an inward-rectifier K^+ channel. *Nature*, **371**, 243–246.

Mackinnon,R. (1991) Determination of the subunit stoichiometry of a voltage-activated potassium channel. *Nature*, **350**, 232–235.

Mackinnon,R. (1995) Pore loops: an emerging theme in ion channel structure. *Neuron*, **14**, 889–892.

Matsuda,H. (1991) Magnesium gating of the inwardly rectifying K^+ channel. *Annu. Rev. Physiol.*, **53**, 289–298.

Nichols,C.G., Makhina,E.N., Pearson,W.L., Sha,Q. and Lopatin,A.N. (1996) Inward rectification and implications for cardiac excitability. *Circ. Res.*, **78**, 1–7.

Pascual,J.M., Shieh,C.C., Kirsch,G.E. and Brown,A.M. (1995) K^+ pore structure revealed by receptor cysteines at inner and outer surfaces. *Neuron*, **14**, 1055–1063.

Pongs,O. (1992) Molecular biology of voltage-dependent potassium channels. *Physiol. Rev.*, **72**, S69–S88.

Pongs,O. (1993) Structure–function studies on the pore of potassium channels. *J. Membr. Biol.*, **136**, 1–8.

Pongs,O. (1995) Regulation of the activity of voltage-gated potassium channels by beta subunits. *Semin. Neurosci.*, **7**, 137–146.

Rehm,H. and Lazdunski,M. (1988) Purification and subunit structure of a putative K^+-channel protein identified by its binding properties for dendrotoxin I. *Proc. Natl Acad. Sci. USA*, **85**, 4919–4923.

Reid,J.D., Lukas,W., Shafaatian,R., Bertl,A., Scheurmann-Kettner,C., Guy,H.R. and North,A. (1996) The *S.cerevisiae* outwardly-rectifying potassium channel (DUK1) identifies a new family of channels with duplicated pore domains. *Receptors Channels*, **4**, 51–62.

Rhodes,K.J., Keilbaugh,S.A., Barrezueta,N.X., Lopez,K.L. and Trimmer,J.S. (1995) Association and colocalization of K^+ channel alpha- and beta-subunit polypeptides in rat brain. *J. Neurosci.*, **15**, 5360–5371.

Rudy,B. (1988) Diversity and ubiquity of K^+ channels. *Neuroscience*, **25**, 729–749.

Ruppersberg,J.P., Schröter,K.H., Sakman,B., Stocker,M., Sewing,S. and Pongs,O. (1990) Heteromultimeric channels formed by rat brain potassium channel protein. *Nature*, **345**, 535–537.

Salkoff,L., Baker,K., Butler,A., Covarrubias,M., Pak,M.D. and Wei,A.G. (1992) An essential set of K^+ channels conserved in flies, mice and humans. *Trends Neurosci.*, **15**, 161–166.

Shen,N.V. and Pfaffinger,P.J. (1995) Molecular recognition and assembly sequences involved in the subfamily-specific assembly of voltage-gated potassium channel subunit proteins. *Neuron*, **14**, 625–633.

Sheng,M., Liao,Y.J., Jan,Y.N. and Jan,L.Y. (1993) Presynaptic A-current based on heteromultimeric K^+ channels detected *in vivo*. *Nature*, **365**, 72–75.

Summers,M.D. and Smith,G.E. (1987) *A Manual of Methods of Baculovirus and Insect Cell Culture Procedures*. Texas Agricultural Experimental Station Bulletin.

Wang,H., Kunkel,D.D., Martin,T.M., Schwartzkroin,P.A. and Tempel, B.L. (1993) Heteromultimeric K^+ channels in terminal and juxtaparanodal regions of neurons. *Nature*, **365**, 75–79.

Xu,J., Yu,W.F., Jan,Y.N., Jan,L.Y. and Li,M. (1995) Assembly of voltage-gated potassium channels—conserved hydrophilic motifs determine subfamily-specific interactions between the alpha-subunits. *J. Biol. Chem.*, **270**, 24761–24768.

Yang,J., Jan,Y.N. and Jan,L.Y. (1995) Determination of the subunit stoichiometry of an inwardly rectifying potassium channel. *Neuron*, **15**, 1441–1447.

Received on July 8, 1996; revised on August 15, 1996